

Martensitic transformation and magnetocaloric effect in $\text{Ni}_{43}\text{Mn}_{42}\text{Co}_4\text{Sn}_{11}$ alloy

FENGHUA CHEN, CHANGWEI GONG^a, YANPING GUO^a, MINGANG ZHANG^{a,*},
YUESHENG CHAI^a, JIAN WEI

Department of Physics, School of Applied Science, TaiYuan University of Science and Technology, Taiyuan 030024, China

^aCollege of Materials Science and Engineering, TaiYuan University of Science and Technology, Taiyuan 030024, China

The crystal structure and phase transition in Heusler alloys were investigated by means of structure analysis and magnetism measurements. The result shows that the $\text{Ni}_{43}\text{Mn}_{42}\text{Co}_4\text{Sn}_{11}$ alloy have a large magnetic entropy change of 40.0 J/kg K at the temperature about 255 K under a magnetic field changing from 0 to 30 kOe. The refrigerant capacity values of the first-order and second-order phase transition under an applied field changing from 0 to 30 kOe are also discussed. The different external magnetic field influence on the phase transition temperature of about 3-4 K, ranged to the low temperature.

(Received February 4, 2013; accepted January 22, 2014)

Keywords: Ni–Mn–Sn, Heusler alloy, Martensitic transition, Magnetocaloric effect

1. Introduction

Martensitic transformations are solid-state first order structural phase transformations which are displacive, diffusionless and dominated by the strain-energy arising from shear-like displacements. In 1997, the discovery of the giant magnetocaloric effect (MCE) at room temperature in $\text{Gd}_5\text{Si}_2\text{Ge}_2$ [1] offered a promising development of economical and environmental-friendly magnetic refrigerants working at near room temperature. More recently, the so-called inverse MCE has been observed near room temperature in martensitic Ni–Mn–Sn Heusler alloys [2] which cool in a magnetic field applied in the martensitic state. For better understand the mechanism of these materials and to design magnetic shape memory materials, a priority program entitled "Change of microstructure and shape of solid materials by external magnetic fields", was supported by the Deutsche Forschungsgemeinschaft (SPP1239) has been established in 2006[3].

In the case of Ni–Mn–Sn system, the austenitic phase has a cubic $L2_1$ structure, like the Ni–Mn–Ga alloys [4], whereas the structure of the martensitic phase can be $10M$, $14M$, $L1_0$, $4O$ depending on composition [5-7]. The characteristic temperatures in ferromagnetic shape memory alloys (FSMAs) of martensitic start temperature (M_s), martensitic finish temperature (M_f), austenitic start temperature (A_s), and austenitic finish temperature (A_f) are all very sensitive to the composition. It was reported that the martensitic transition (MT) temperatures increase with the increasing value of valence electron density (e/a), which was further confirmed by the experimental results in

Co, Fe, Ge, B, Al, Si and Cu doped Ni–Mn–Sn alloys [8-20].

In this work, we substituted Mn with Co in $\text{Ni}_{43}\text{Mn}_{42}\text{Co}_4\text{Sn}_{11}$ alloys, and investigated the phase transition and magnetocaloric effect in these alloys. The different external magnetic field influence on the phase transition temperature also investigated.

2. Experimental

The polycrystalline ingots of nominal compositions $\text{Ni}_{43}\text{Mn}_{42}\text{Co}_4\text{Sn}_{11}$ alloys were prepared by arc melting the required amount of constituent high purity elements (99.98% purity) in a cold copper crucible under argon atmosphere. For homogenization, the samples were flipped and re-melted. The ingots were cut into small pieces and annealed at 1173 K for 48 h in vacuum quartz tubes, then quenched in ice water. Microstructure and elemental compositions of the samples were investigated by field emission scanning electron microscopy (FE-SEM, Hitachi S-4800) attached with an X-ray energy dispersive spectroscopy (EDS, Thermo System 7) setup. The crystal structure of the sample was analyzed using Panalytical X'Pert PRO type X-ray diffractometer with $\text{Cu } K\alpha$ radiation at room temperature. The magnetic properties were measured using a Quantum Design's multi-use vibrating sample magnetometer VersaLab system under a magnetic field up to 30 kOe.

3. Results and discussion

Fig. 1 shows the XRD patterns of $\text{Ni}_{43}\text{Mn}_{42}\text{Co}_4\text{Sn}_{11}$ alloys at room temperature. The diffraction peaks in the samples were indexed. All the peaks correspond to the Heusler $L2_1$ cubic structure, indicates that the samples are in austenitic phase and the MT temperatures are below room temperature.

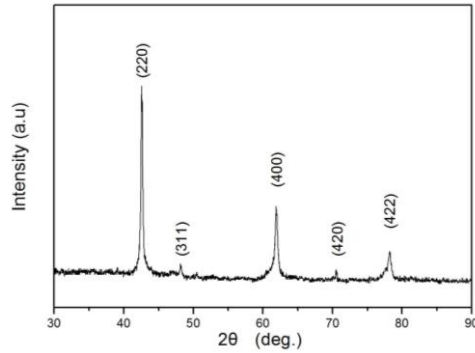
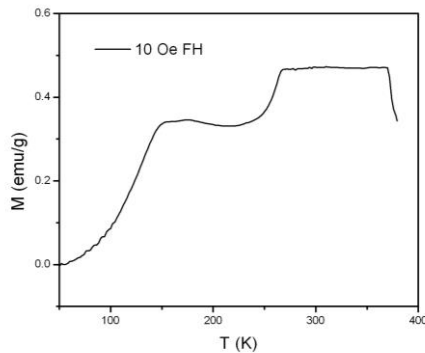
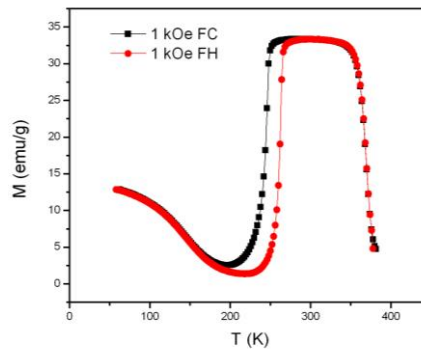


Fig. 1. The XRD patterns of $\text{Ni}_{43}\text{Mn}_{42}\text{Co}_4\text{Sn}_{11}$ alloys at room temperature.



(a)



(b)

Fig. 2. (Color online) The temperature dependence of magnetization M - T curves for $\text{Ni}_{43}\text{Mn}_{42}\text{Co}_4\text{Sn}_{11}$ alloys on heating and cooling under a magnetic field of 10 Oe (a) and 1 kOe (b).

Isothermal magnetization curves M - H for $\text{Ni}_{43}\text{Mn}_{42}\text{Co}_4\text{Sn}_{11}$ alloys were measured near the MT temperatures. Fig. 3 show the M - H curves for $\text{Ni}_{43}\text{Mn}_{42}\text{Co}_4\text{Sn}_{11}$ with a field up to 30 kOe. The typical metamagnetic behavior, due to the field-induced MT , can be observed in this plot. The magnetization changed about 80 emu/g, within the temperature about 20 K. The metamagnetic character in the M - H isotherms is associated with a field-induced reverse martensitic transformation from a low magnetization martensitic state to a higher magnetization austenite state.

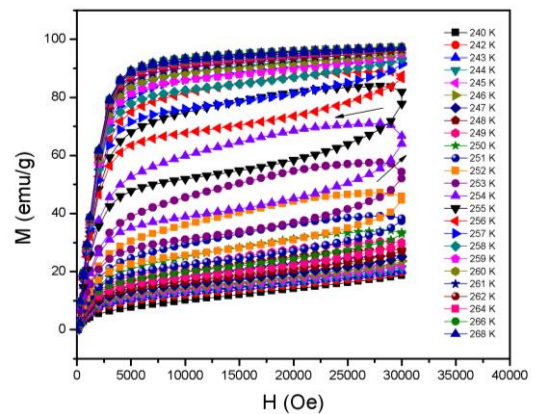


Fig. 3. (Color online) Isothermal magnetization curves of $\text{Ni}_{43}\text{Mn}_{42}\text{Co}_4\text{Sn}_{11}$ alloys measured in various temperatures.

The temperature dependence of the magnetization M - T curves for the $\text{Ni}_{43}\text{Mn}_{42}\text{Co}_4\text{Sn}_{11}$ alloys were measured. Fig. 2 shows M - T curves for $\text{Ni}_{43}\text{Mn}_{42}\text{Co}_4\text{Sn}_{11}$ on heating and cooling in a magnetic field of 10 Oe and 1 kOe. A thermal hysteresis about 20 K is obviously observed around the MT temperature, while no thermal hysteresis is observed near the Curie temperature of austenitic phase (T_c^A). Between the martensitic transition and the reverse martensitic transition, there is an obvious thermal hysteresis, which is attributed to a first-order structural transition. The M_s at about 248 K, M_f at about 225 K, A_s at about 246 K, and A_f at about 266 K, which are estimated from M - T curves.

The MCE ΔS_M was calculated from the isothermal magnetization curves using the Maxwell equation[21]:

$$\Delta S_M(T, H) = \int_0^H \left(\frac{\partial M(T, H)}{\partial T} \right)_H dH$$

The temperature dependence of ΔS_M in applied fields (ΔH) of 10, 20 and 30 kOe for $\text{Ni}_{43}\text{Mn}_{42}\text{Co}_4\text{Sn}_{11}$ are show in Fig. 4. The maximum values of ΔS_M is 40.0 J/kg K for applied field at 30 kOe. Even at the (ΔH) of 10 kOe, we still get the ΔS_M of 12.6 J/kg K.

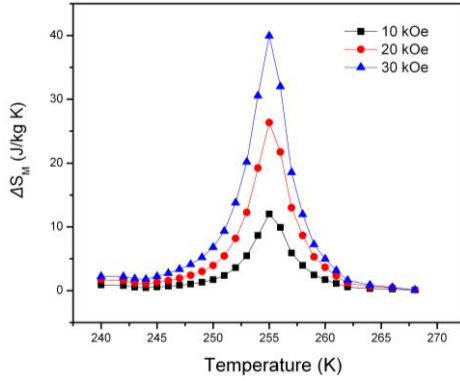


Fig. 4. (Color online) The temperature dependence of ΔS_M in the magnetic field of 10, 20, and 30 kOe for $\text{Ni}_{43}\text{Mn}_{42}\text{Co}_4\text{Sn}_{11}$ alloys.

In order to better study the applied magnetic field influence of the phase transition temperature of the alloy, the phase transition temperature range of different applied magnetic field have been tested. Fig. 5 shows the temperature dependence of magnetization M - T curves for $\text{Ni}_{43}\text{Mn}_{42}\text{Co}_4\text{Sn}_{11}$ alloy on heating and cooling under magnetic field of 10, 20, and 30 kOe. The different external magnetic field influence on the phase transition temperature of about 4-5 K/10 kOe, ranged to the low temperature. The study for further promote the application of magnetic refrigeration is a useful attempt.

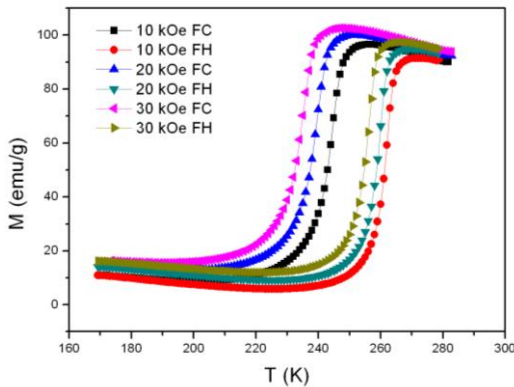


Fig. 5. (Color online) The temperature dependence of magnetization M - T curves for $\text{Ni}_{43}\text{Mn}_{42}\text{Co}_4\text{Sn}_{11}$ alloy on heating and cooling under magnetic field of 10, 20, and 30 kOe.

Isothermal magnetization curves M - H for $\text{Ni}_{43}\text{Mn}_{42}\text{Co}_4\text{Sn}_{11}$ alloy were measured near the Curie temperature of austenitic phase (T_c^A). Fig. 6 show the M - H curves for $\text{Ni}_{43}\text{Mn}_{42}\text{Co}_4\text{Sn}_{11}$ with a field up to 30 kOe. The magnetization changed about 30 emu/g, within the temperature changed about 40 K.

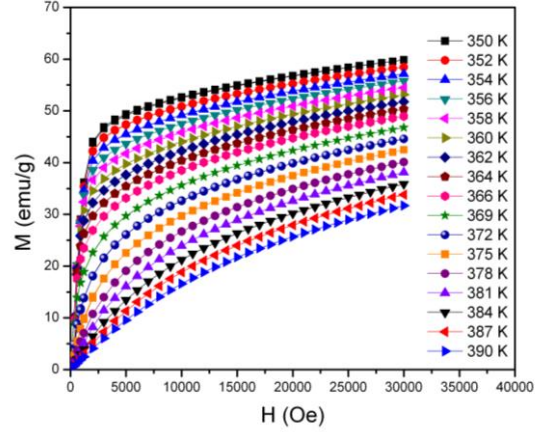


Fig. 6. (Color online) Isothermal magnetization curves of $\text{Ni}_{43}\text{Mn}_{42}\text{Co}_4\text{Sn}_{11}$ alloy measured in various temperatures at near the T_c^A .

The temperature dependence of ΔS in applied fields (ΔH) of 10, 20 and 30 kOe for $\text{Ni}_{43}\text{Mn}_{42}\text{Co}_4\text{Sn}_{11}$ are showed in Fig. 7. The maximum values of ΔS is -2.85 J/kg K for applied field at 30 kOe. Even at the (ΔH) of 10 kOe, we still get the ΔS of -1.2 J/kg K.

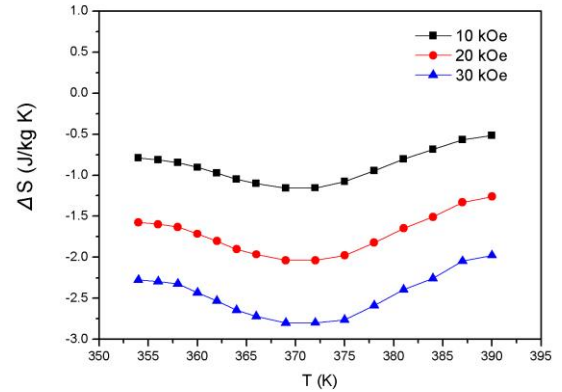


Fig. 7. (Color online) The temperature dependence of ΔS at near the Curie temperature of austenitic phase (T_c^A) in the magnetic field of 10, 20, and 30 kOe for $\text{Ni}_{43}\text{Mn}_{42}\text{Co}_4\text{Sn}_{11}$ alloy.

The refrigerant capacity (RC), an important parameter to evaluate MCE, which is a measurement of the heat transferred between the cold and hot reservoirs in an ideal refrigeration cycle [22,23]. RC values are usually determined by numerically integrating the ΔS_M - T curves over the full width at half maximum. With the field changing from 0 to 30 kOe, the RC value of $\text{Ni}_{43}\text{Mn}_{42}\text{Co}_4\text{Sn}_{11}$ alloy of the first-order transition and

second-order transition are 121.8 J/kg and -152.3 J/kg.

4. Conclusion

The component dependence of MT and ΔS_M in Ni₄₃Mn₄₂Co₄Sn₁₁ alloy were investigated. The large ΔS_M in a low field of 10 kOe, and 20 kOe were 12.6 J/kg K and 27.1 J/kg K, and a large magnetic entropy change of 40.0 J/kg K obtained in a field changing from 0 to 30 kOe. The large magnetic entropy change can be ascribes to the abrupt change of magnetization in the vicinity of MT temperatures. The large ΔS_M adjustable MT temperatures, and the low cost suggest Ni₄₃Mn₄₂Co₄Sn₁₁ alloy as promising working substances for magnetic refrigeration. With the field changing from 0 to 30 kOe, the refrigerant capacity(RC) value of Ni₄₃Mn₄₂Co₄Sn₁₁ alloy for the first-order and second-order phase transition are 121.8 J/kg and -152.3 J/kg.

Acknowledgements

This work was supported by Natural Science Foundation of Shanxi Province of China (Grants No.2010011032-1), Specialized Research Fund for Doctoral Scientific Research of Ministry of Education of China (Grants No. 201014151110003), Doctoral Scientific Research Foundation of Taiyuan University of Science and Technology (Grants No. 20122036), University students Innovation Project of Taiyuan University of Science and Technology (Grants No. xj2013073), Graduate student Innovation Project of Shanxi Province (Grants No. 20133114), Research Project Supported by Shanxi Scholarship Council of China (2013-098), National Natural Science Foundation of China (Grants No. 61178067).

References

- [1] V. K. Pecharsky, K. A. Gschneider Jr, Phys. Rev. Lett. **78**, 4494 (1997).
- [2] T. Krenke, E. Duman, M. Acet, E. F. Wassermann, X. Moya, L. Mañosa, A. Planes, Nat. Mater. **4**, 450 (2005).
- [3] <http://www.magneticshape.de/>.
- [4] A. Sozinov, A. A. Likhachev, N. Lanska, K. Ullakko, Appl. Phys. Lett. **80**, 1746 (2002).
- [5] P. J. Brown, A. P. Gandy, K. Ishida, R. Kainuma, T. Kanomata, K. U. Neumann, K. Oikawa, B. Ouladdiaf, K. R. A. Ziebeck, J. Phys.: Condens. Matter **18**, 2249 (2006).
- [6] K. Koyama, K. Watanabe, T. Kanomata, R. Kainuma, K. Oikawa, K. Ishida, Appl. Phys. Lett. **89**, 132505 (2006).
- [7] T. Krenke, M. Acet, E. F. Wassermann, X. Moya, L. Mañosa, A. Planes, Phys. Rev. B **72**, 014412 (2005).
- [8] T. Krenke, E. Duman, M. Acet, X. Moya, L. Manosa, A. Planes, J. Appl. Phys. **102**, 033903 (2007).
- [9] S. Aksoy, T. Krenke, M. Acet, E.F. Wassermann, X. Moya, L. Mañosa, A. Planes, Appl. Phys. Lett. **91**, 241916 (2007).
- [10] H. C. Xuan, D. H. Wang, C. L. Zhang, Z. D. Han, B. X. Gu, Y. W. Du, Appl. Phys. Lett. **92**, 102503 (2008).
- [11] I. Dincer, E. Yüzüak, Y. Elerman, J. Alloy. Compd. **506**, 508 (2010).
- [12] Liu Zhuhong, Wu Zhigang, Yang Hong, Liu Yinong, Wang Wenhong, Ma Xingqiao, Wu Guangheng, Intermetallics **19**, 1605 (2011).
- [13] Z. Li, C. Jing, H. L. Zhang, Y. F. Qiao, S. X. Cao, J. C. Zhang, L. Sun, J. Appl. Phys. **106**, 083908 (2009).
- [14] A. K. Nayak, K. G. Suresh, A. K. Nigam, J. Appl. Phys. **107**, 09A927 (2010).
- [15] Z. D. Han, D. H. Wang, C. L. Zhang, H. C. Xuan, J. R. Zhang, B. X. Gua, Y. W. Du, Mater. Sci. Eng. B **157**, 40 (2009).
- [16] V. K. Sharma, M. K. Chattopadhyay, S. B. Roy, J. Phys. D: Appl. Phys. **43**, 225001 (2010).
- [17] R. L. Wang, J. B. Yan, H. B. Xiao, L. S. Xu, V. V. Marchenkov, L. F. Xu, C. P. Yang, J. Alloy. Compd. **509**, 6834 (2011).
- [18] J. Chen, Z. D. Han, B. Qian, P. Zhang, D. H. Wang, Y. W. Du, J. Magn. Magn. Mater. **323**, 248 (2011).
- [19] T. F. Zheng, Y. G. Shi, C. C. Hu, J. Y. Fan, D. N. Shi, S. L. Tang, Y. W. Du, J. Magn. Magn. Mater. **324**, 4102 (2012).
- [20] Y. G. Shi, L. S. Xu, X. G. Zhou, Z. Y. Chen, T. F. Zheng, D. N. Shi, Phys Status Solidi A DOI:10.1002/pssa.201330071 (2013).
- [21] T. Krenke, E. Duman, M. Acet, E. F. Wassermann, X. Moya, L. Mañosa, A. Planes, Nat. Mater. **4**, 450 (2005).
- [22] K. A. Gschneider Jr., V. K. Pecharsky, A. O. Pecharsky, C. B. Zimm, Mater. Sci. Forum **315**, 69 (1999).
- [23] K. A. Gschneider Jr., V. K. Pecharsky, A. O. Tsokol, Rep. Prog. Phys. **68**, 1479 (2005).

*Corresponding author: phycfh@163.com, mgzhang@163.com